

Spectroelectrochemical Identification of a Pentavalent Uranyl Tetrachloro Complex in Room-Temperature Ionic Liquid

Toshinari Ogura,[†] Koichiro Takao,[‡] Kotoe Sasaki,^{†,§} Tsuyoshi Arai,[§] and Yasuhisa Ikeda^{*,†}[†]Research Laboratory for Nuclear Reactors, Tokyo Institute of Technology, Tokyo, Japan[‡]Department of Materials and Life Science, Seikei University, Tokyo, Japan[§]Shibaura Institute of Technology, Tokyo, Japan

S Supporting Information

ABSTRACT: Reduction of $U^{VI}O_2Cl_4^{2-}$ in a mixture of 1-ethyl-3-methylimidazolium tetrafluoroborate and its chloride at $E^{o'} = -0.996$ V vs Fc/Fc⁺ and 298 K affords $U^VO_2Cl_4^{3-}$, which is kinetically stable and exhibits typical character of U^V in the UV–vis–NIR absorption spectrum.

The redox chemistry of $U^{VI}O_2^{2+}$ in molten salts is of great interest not only for its basic chemistry but also for the pyrochemical reprocessing of spent nuclear fuels. In most cases, chloride melts were used, where $U^{VI}O_2^{2+}$ is regarded to form a stable tetrachloro complex $U^{VI}O_2Cl_4^{2-}$.¹ The reduction product of $U^{VI}O_2Cl_4^{2-}$ is believed to be the corresponding tetrachloro uranyl(V) species, $U^VO_2Cl_4^{3-}$, which was derived by the recent extended X-ray absorption fine structure (EXAFS) studies.^{1f,g} The occurrence of this uranium(V) species is also of special interest in uranium(V) chemistry, which attracts attention in recent actinide chemistry because of the limited investigation of its instability.² The electronic absorption spectrum of $U^VO_2Cl_4^{3-}$ is of U^{5+} in D_{4h} symmetry, which is another system involving the inversion center (cf. $U^{VO_2}(CO_3)_3^{5-}$ in D_{6h}) and a good sample to corroborate the relationship between the coordination structure around U^{5+} and the spectroscopic properties directly related to the Laporte selection rule.^{2d,e}

Although the melting points of the salts used as media in the former publications¹ are different, the experiments were performed generally at several hundreds to ca. 1000 K. This condition is, however, very extreme and not always easy to handle. Ionic liquids (ILs) melt “around” room temperature. Hence, the use of this medium is one of the selections to drastically reduce the experimental temperature for ease of handling. Starting from a Cl^- -based IL is a simple way to mimic the high-temperature chloride melts, and as a matter of fact, there are several related reports regarding the electrochemistry of $U^{VI}O_2^{2+}$.^{3,4} However, most Cl^- salts of typical cations of ILs (e.g., N,N' -dialkylimidazolium, N -alkylpyridinium) are solid at room temperature, and even if they melt with gentle heating, they are so viscous that their handling is still difficult.

In order to overcome these points and to facilitate the “real” room-temperature experiments, a mixed salt system was used in this study; 1-ethyl-3-methylimidazolium chloride (EMI^+Cl^-) was mixed with the tetrafluoroborate of the same cation ($EMI^+BF_4^-$) in a 50:50 mol % ratio. The BF_4^- counteranion to EMI^+ was selected because this anion is expected not to affect the coordination of the metal ion. To study the redox behavior of

$U^{VI}O_2^{2+}$ in the $EMI^+BF_4^-/Cl^-$ melt, we performed cyclic voltammetry (CV) experiments. Although similar works have already been done in EMI^+ or N - n -butylpyrinium halides/ AlX_3 ($X = Cl, Br$)³ and 1-butyl-3-methylimidazolium chloride,⁴ only the current–potential curve from CV and related electrochemical experiments were reported and no quantitative evidence for speciation in the studied systems was provided. Herein we succeeded in identification of the reduction product of U^{VI} in our system and obtaining its spectroscopic data by UV–vis–NIR spectroelectrochemical technique using an optical transparent thin-layer electrode (OTTLE) cell (Figure S1).⁵

In the UV–vis absorption spectrum of the $EMI^+BF_4^-/Cl^-$ solution dissolving $(EMI)_2U^{VI}O_2Cl_4$ (Figure S2 in the Supporting Information), the uranyl ion shows a finely structured absorption spectrum around 430 nm, which is characteristic of $U^{VI}O_2Cl_4^{2-}$.⁶ As a matter of fact, the virtually identical spectrum of $U^{VI}O_2Cl_4^{2-}$ was also observed in other IL systems.^{6,7} Cyclic voltammograms of $U^{VI}O_2Cl_4^{2-}$ in $EMI^+BF_4^-/Cl^-$ at different potential sweep rates (ν) are shown in Figure 1. Coupled reduction and oxidation waves were found around -1.05 (E_{pc}) and -0.92 V (E_{pa}), respectively. Any successive reactions after reduction of $U^{VI}O_2Cl_4^{2-}$ seem not to occur because identical voltammograms were observed in multiple CV scans. The separation between the reduction and oxidation peaks increases from 0.101 to 0.152 V as ν increases. These facts suggest that the redox reaction of $U^{VI}O_2Cl_4^{2-}$ is quasi-reversible. The formal potential $E^{o'}$ $[=(E_{pc} + E_{pa})/2]$ is almost constant at -0.989 ± 0.002 V regardless of ν .⁸ The reduction product should be considered to be the corresponding uranium(V) species, $U^VO_2Cl_4^{3-}$, for the following reasons: (i) quasi-reversible cyclic voltammograms imply no large structure modification, e.g., addition/elimination of Cl^- to/from the “ UO_2Cl_4 ” unit; (ii) if uranium(IV) is formed, insoluble $U^{IV}O_2$ will deposit on the electrode surface, which alters the electrode character, resulting in no reproducible voltammograms in the multiple-scan experiment; (iii) to generate a soluble uranium(IV), the axial oxygen atoms originating to $U^{VI}O_2^{2+}$ have to be removed through protonation or reaction with a Lewis acid such as $Al_2Cl_7^-$. However, any reactive species are present in the current system. This is also the case when disproportionation of $U^VO_2^+$ is neglected.^{2c–e}

This qualitative conclusion should be corroborated quantitatively. We performed the UV–vis–NIR spectroelectrochemical

Received: July 25, 2011

Published: October 04, 2011

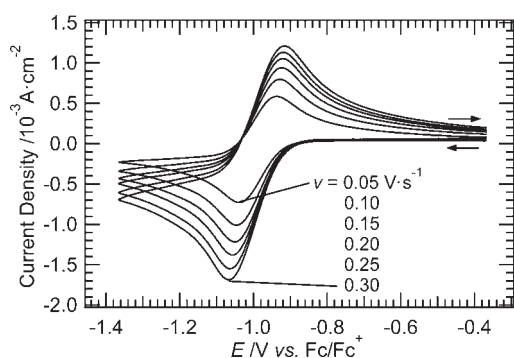


Figure 1. Cyclic voltammograms of $\text{U}^{\text{VI}}\text{O}_2\text{Cl}_4^{2-}$ (6.06×10^{-2} M) in $\text{EMI}^+\text{BF}_4^-/\text{Cl}^-$ (50:50 mol %) at 298 K and different potential sweep rates (v).

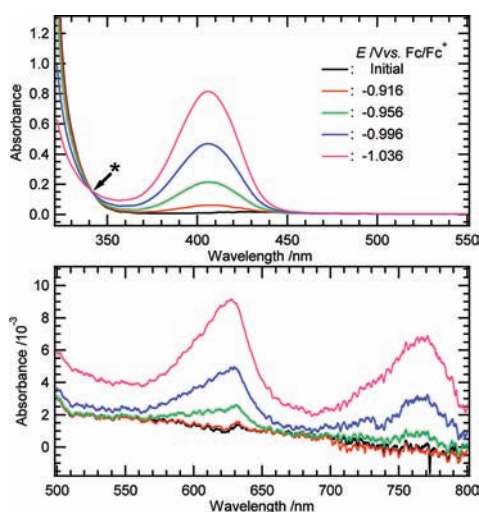


Figure 2. UV-vis-NIR absorption spectra of a $\text{EMI}^+\text{BF}_4^-/\text{Cl}^-$ 50:50 mol % solution dissolved $(\text{EMI})_2\text{U}^{\text{VI}}\text{O}_2\text{Cl}_4$ (5.48×10^{-2} M in total) at 298 K and different potentials. Wavelength range: 320–550 nm (upper); 500–800 nm (lower). The asterisk indicates the isosbestic point at 342 nm.

experiment for $\text{U}^{\text{VI}}\text{O}_2\text{Cl}_4^{2-}$ in $\text{EMI}^+\text{BF}_4^-/\text{Cl}^-$. The resulting spectra recorded at different potentials (E) are shown in Figure 2. With decreasing potential, an intense peak appears with a maximum at 406 nm. A similar absorption band was also observed by Nagai et al.^{1d} Furthermore, much weaker absorption bands were also found at 630 and 770 nm, where $\text{U}^{\text{VI}}\text{O}_2\text{Cl}_4^{2-}$ has no absorption. These spectral changes were observed in the presence of an isosbestic point at 342 nm, indicating that only the redox equilibrium of $\text{U}^{\text{VI}}\text{O}_2\text{Cl}_4^{2-}$ is present in the E range of Figure 2. When $E < -1.036$ V, the observed spectrum no longer passed through the isosbestic point, meaning that another reaction like degradation of the U^{V} species took place. This undesired reaction was not detected up to -1.366 V in the CV experiment (Figure 1), and therefore its reaction rate seems to be much slower than the CV time scale (ca. 10^1 s) but similar to that of wavelength scanning in the UV-vis-NIR absorption spectra recording (ca. 1 h in total). The uranium(V) species, $\text{U}^{\text{V}}\text{O}_2\text{Cl}_4^{3-}$, is likely to be, at least, kinetically stable in the current system.

The spectral changes observed in Figure 2 do not reach completion of the reduction. However, it is still possible to discuss its reaction mechanism using the Nernst equation. Concentrations

of oxidant (C_{O}) and reductant (C_{R}) can be expressed by

$$C_{\text{O}} = C_{\text{total}} / \left[1 + \exp\left(\frac{nF}{RT}(E^{\circ'} - E)\right) \right] \quad (1)$$

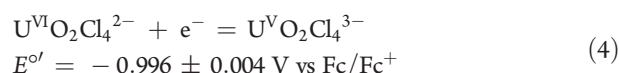
$$C_{\text{R}} = C_{\text{total}} / \left[1 + \exp\left(\frac{nF}{RT}(E - E^{\circ'})\right) \right] \quad (2)$$

where $C_{\text{total}} = C_{\text{O}} + C_{\text{R}}$. The electron stoichiometry, Faraday constant, gas constant, absolute temperature, and formal potential are denoted by n , F , R , T , and $E^{\circ'}$, respectively. According to Beer's law, the observed absorbance (A) is given by $A = (\varepsilon_{\text{O}}C_{\text{O}} + \varepsilon_{\text{R}}C_{\text{R}})l$, where ε and l are the molar absorptivity of the species (subscripts O and R indicate oxidant and reductant) and optical path length, respectively. Therefore,

$$A = \left\{ \left[\varepsilon_{\text{O}} + \varepsilon_{\text{R}} \exp\left(\frac{nF}{RT}(E^{\circ'} - E)\right) \right] / \left[1 + \exp\left(\frac{nF}{RT}(E^{\circ'} - E)\right) \right] \right\} C_{\text{total}}l \quad (3)$$

The molar absorptivity ε_{O} of $\text{U}^{\text{VI}}\text{O}_2\text{Cl}_4^{2-}$, C_{total} , F , R , T , and l are already known. The electron stoichiometry n must be an integer. We set $n = 1, 2, \dots$ and performed the least-squares regression with unknown parameters ε_{R} and $E^{\circ'}$ to find the best reproduction of the experimental points. As a result, the best fit was obtained as shown in Figure S3, where $n = 1$ and the point before the E application was expediently put at -0.80 V, where $\text{U}^{\text{VI}}\text{O}_2\text{Cl}_4^{2-}$ is eventually predominant and its reduction can be ignored. When $n \geq 2$, the fits largely deviated from the experimental points and resulted in greater χ^2 (Figure S4), indicating that the wrong n was set.

Consequently, the following one-electron reduction of $\text{U}^{\text{VI}}\text{O}_2\text{Cl}_4^{2-}$ affording $\text{U}^{\text{V}}\text{O}_2\text{Cl}_4^{3-}$ in $\text{EMI}^+\text{BF}_4^-/\text{Cl}^-$ was elucidated.



The value of $E^{\circ'}$ is also consistent with that derived from the CV data (Figure 1). As described above, slow degradation of $\text{U}^{\text{V}}\text{O}_2\text{Cl}_4^{3-}$ was found in the current system, and the spectrum recorded at the lowest E in Figure 2 (-1.036 V) is of an admixture of $\text{U}^{\text{VI}}\text{O}_2\text{Cl}_4^{2-}$ and $\text{U}^{\text{V}}\text{O}_2\text{Cl}_4^{3-}$. Nevertheless, the characteristic absorption bands of $\text{U}^{\text{V}}\text{O}_2\text{Cl}_4^{3-}$ were confirmed in the vis-NIR region and are common to uranium(V). The wavelengths of absorption maxima and ε values normalized by the Nernstian profile of $C_{\text{R}}/C_{\text{total}}$ at -1.036 V ($C_{\text{O}}/C_{\text{total}}:C_{\text{R}}/C_{\text{total}} = 0.174:0.826$) are summarized in Table 1 together with those of the uranium(V) species in high-temperature chloride melts and in different symmetries.^{1,2d,2e} The current result compares well with the previous reports. The coordination structure around the $\text{U}^{\text{V}}\text{O}_2^+$ ion in the high-temperature melts was supposed to be $\text{U}^{\text{V}}\text{O}_2\text{Cl}_4^{3-}$ only on the basis of the EXAFS data,^{1fg} while the CV and spectroelectrochemical experiments in this study clarified that the reduction product of $\text{U}^{\text{VI}}\text{O}_2\text{Cl}_4^{2-}$ in $\text{EMI}^+\text{BF}_4^-/\text{Cl}^-$ is certainly $\text{U}^{\text{V}}\text{O}_2\text{Cl}_4^{3-}$. Therefore, the uranium(V) species in the chloride melts of the previous works¹ are also likely to be the tetrachloro complex proposed. Unfortunately, further characteristics of $\text{U}^{\text{V}}\text{O}_2\text{Cl}_4^{3-}$ at $\lambda > 800$ nm were not be able to be studied because of strong absorption by $\text{EMI}^+\text{BF}_4^-/\text{Cl}^-$. However, the small ε values listed in Table 1 are strongly indicative of the forbidden transition in $\text{U}^{\text{V}}\text{O}_2^+$ immersed in D_{4h} symmetry, where there is an inversion center, as discussed in

Table 1. Wavelengths (λ_{abs}) and Molar Absorptivities (ϵ) of Absorption Maxima of $\text{U}^{\text{V}}\text{O}_2\text{Cl}_4^{3-}$ in $\text{EMI}^+\text{BF}_4^-/\text{Cl}^-$ at 298 K and Uranium(V) Species in High-Temperature Chloride Melts together with Corresponding Data for Related $\text{U}^{\text{V}}\text{O}_2^+$ Species in Different Symmetries

| uranium(V) species ^a | symmetry | solvent | T/K | $\lambda_{\text{abs}}/\text{nm}$ ($\epsilon/\text{M}^{-1}\cdot\text{cm}^{-1}$) | | ref |
|--|----------|--|------|--|------------|-----------|
| $\text{U}^{\text{V}}\text{O}_2\text{Cl}_4^{3-}$ | D_{4h} | $\text{EMI}^+\text{BF}_4^-/\text{Cl}^-$ ^b | 298 | 630 (9.5) | 770 (7.1) | this work |
| UO_2^+ | - | $\text{LiCl}-\text{KCl}$ ^c | 923 | 625 (8.8) | 800 (15.2) | 1b |
| UO_2^+ | - | $\text{LiCl}-\text{KCl}$ ^c | 1023 | 625 (6) | 800 (11) | 1b |
| UO_2^+ | - | $\text{LiCl}-\text{KCl}$ ^d | 923 | 625 (9.9) | 800 (17.1) | 1b |
| UO_2^+ | - | $\text{NaCl}-\text{KCl}-\text{MgCl}_2$ ^c | 923 | 685 (5.6) | 860 (8.9) | 1b |
| UO_2^+ | - | $\text{CsCl}-\text{NaCl}$ | 940 | 615 | 770 | 1c |
| UO_2^+ | - | $\text{NaCl}-\text{KCl}$ | 940 | 615 | 770 | 1c |
| UO_2^+ | - | $\text{NaCl}-2\text{CsCl}$ | 923 | 620 (12.5) | 775 (15.9) | 1d |
| $[\text{U}^{\text{V}}\text{O}_2(\text{salophen})\text{DMSO}]^{-e}$ | D_{5h} | DMSO | 298 | 650 (140) | 750 (220) | 2d |
| $[\text{U}^{\text{V}}\text{O}_2(\text{dbm})_2\text{DMSO}]^{-f}$ | D_{5h} | DMSO | 298 | 640 (400) | 740 (800) | 2d |
| $[\text{U}^{\text{V}}\text{O}_2(\text{saldien})]^{-g}$ | D_{5h} | DMSO | 298 | 630 (300) | 700 (400) | 2e |
| $[\text{U}^{\text{V}}\text{O}_2(\text{CO}_3)_3]^{5-}$ | D_{6h} | 1 M $\text{Na}_2\text{CO}_3(\text{aq})$ | 298 | 760 (2.0) | 990 (2.8) | 2d |

^a Notation follows that represented in the corresponding reference. ^b 50:50 mol %. ^c Eutectic. ^d 70:30 mol %. ^e salophen = N,N' -disalicylidene-*o*-phenylenediamine. ^f dbm = dibenzoylmethane. ^g saldien = N,N' -disalicylidenediethylenetriamine.

our former articles.^{2d,e} The Laporte forbiddenness implies that these absorption bands arise from the metal-centered $f-f$ transitions in the $5f^1$ configuration of uranium(V) and/or a ligand-to-metal charge-transfer (LMCT) transition from the axial O to $\text{U}^{2d,e,9}$. The more intense band at 406 nm with $\epsilon = 837 \pm 43 \text{ M}^{-1}\cdot\text{cm}^{-1}$ is also intrinsic to $\text{U}^{\text{V}}\text{O}_2\text{Cl}_4^{3-}$ and no longer forbidden even in the strictly regular D_{4h} symmetry of this species. Both the peak wavelength and ϵ value are in good agreement with those in the former report (395 nm and $832 \pm 32 \text{ M}^{-1}\cdot\text{cm}^{-1}$).^{1d} Taking into account that both electronic transitions of $f-f$ and LMCT in the $\text{U}^{\text{V}}\text{O}_2^+$ moiety are forbidden under the presence of an inversion center, the remaining possibility is only those related to the equatorial coordination; i.e., CT between U and Cl. Pentavalent uranium is able to give its f electron to Cl^- , while uranium(VI) cannot because of its radon-like closed shell and no unpaired electrons. Therefore, the direction of charge transfer could be from U to Cl, i.e., MXCT.

■ ASSOCIATED CONTENT

S Supporting Information. Experimental details with a schematic view of the OTTLE cell, UV-vis absorption spectrum of $\text{U}^{\text{VI}}\text{O}_2\text{Cl}_4^{2-}$ in $\text{EMI}^+\text{BF}_4^-/\text{Cl}^-$, absorbance profile at 406 nm of Figure 2, and the best-fit curves of eq 3 when $n = 1, 2, 3$. This material is available free of charge via the Internet at <http://pubs.acs.org>.

■ AUTHOR INFORMATION

Corresponding Author

*E-mail: yiked@nr.titech.ac.jp.

■ REFERENCES

(1) (a) Adams, M. D.; Wenz, D. A.; Steunenberg, R. K. *J. Phys. Chem.* **1963**, *67*, 1939–1941. (b) Wenz, D. A.; Adams, M. D.; Steunenberg, R. K. *Inorg. Chem.* **1964**, *3*, 989–992. (c) Khokhryakov, A. A. *Radiochemistry (Moscow, Russ. Fed.)* **1998**, *40*, 413–415. (d) Nagai, T.; Fujii, T.; Shirai, O.; Yamana, H. *J. Nucl. Sci. Technol.* **2004**, *41*, 690–695. (e) Nagai, T.; Uehara, A.; Fujii, T.; Shirai, O.; Yamana, H. *J. Nucl. Sci. Technol.* **2006**, *43*, 1511–1516. (f) Volkovich, V. A.; May, I.; Sharrad, C. A.; Kinoshita, H.; Polovov, I. B.; Bhatt, A. I.; Charnock, J. M.; Griffiths, T. R.; Lewin, R. G. *Recent Adv. Actinide Sci.* **2006**, 485–490. (g) Volkovich, V. A.; Polovov, I. B.; Vasin, B. D.; Griffiths, T. R.; Sharrad, C. A.; May, I.; Charnock, J. M. *Z. Naturforsch.* **2007**, *62a*, 671–676. (h) Volkovich, V. A.

Aleksandrov, D. E.; Griffiths, T. R.; Vasin, B. D.; Khabibullin, T. K.; Maltsev, D. S. *Pure Appl. Chem.* **2010**, *82*, 1701–1717.

(2) (a) Grenthe, I.; Fuger, J.; Konings, R. J. M.; Lemire, R. J.; Muller, A. B.; Nguyen-Trung, C.; Wanner, H. *Chemical Thermodynamics of Uranium*; OECD/NEA and North-Holland: Amsterdam, The Netherlands, 1992. (b) Gindler, J. E. *The Radiochemistry of Uranium*; Los Alamos Scientific Laboratory, Los Alamos, NM, 1972. (c) Mizuoka, K.; Kim, S.-Y.; Hasegawa, M.; Hoshi, T.; Uchiyama, G.; Ikeda, Y. *Inorg. Chem.* **2003**, *42*, 1031–1038. (d) Mizuoka, K.; Tsushima, S.; Hasegawa, M.; Hoshi, T.; Ikeda, Y. *Inorg. Chem.* **2005**, *44*, 6211–6218. (e) Takao, K.; Kato, M.; Takao, S.; Nagasawa, A.; Bernhard, G.; Hennig, C.; Ikeda, Y. *Inorg. Chem.* **2010**, *49*, 2349–2359 and references cited therein.

(3) (a) De Waele, R.; Heerman, L.; D'olieslager, W. *J. Electroanal. Chem.* **1982**, *142*, 137–146. (b) Heerman, L.; De Waele, R.; D'olieslager, W. *J. Electroanal. Chem.* **1985**, *193*, 289–294. (c) Costa, D. A.; Smith, W. H. *Electrochem. Soc. Proc.* **1998**, 98–11, 266–277. (d) Anderson, C. J.; Choppin, G. R.; Pruett, D. J.; Costa, D.; Smith, W. *Radiochim. Acta* **1999**, *84*, 31–36. (e) Deetlefs, M.; Hussey, C. L.; Mohammed, T. J.; Seddon, K. R.; van den Berg, J.-A.; Zora, J. A. *Dalton Trans.* **2006**, 2334–2341.

(4) (a) Girdhar, P.; Venkatesan, K. A.; Subramaniam, S.; Srinivasan, T. G.; Vasudeva Rao, P. R. *Radiochim. Acta* **2006**, *94*, 415–420. (b) Giridhar, P.; Venkatesan, K. A.; Srinivasan, T. G.; Vasudeva Rao, P. R. *Electrochim. Acta* **2007**, *52*, 3006–3012. (c) Asanuma, N.; Harada, M.; Yasuike, Y.; Nogami, M.; Suzuki, K.; Ikeda, Y. *J. Nucl. Sci. Technol.* **2007**, *44*, 368–372.

(5) (a) Heineman, W. R. *J. Chem. Educ.* **1983**, *60*, 305–308. (b) Endo, A.; Mochida, I.; Shimizu, K.; Sato, G. P. *Anal. Sci.* **1995**, *11*, 457–459. (c) Kaim, W.; Klein, A. *Spectroelectrochemistry*; Royal Society of Chemistry, London, 2008. (d) Bard, A. J.; Faulkner, L. R. *OTTLE: Optical Transparent Thin-Layer Electrode. Electrochemical Methods, Fundamentals and Applications*, 2nd ed.; John Wiley & Sons, Inc.: New York, 2001.

(6) Dai, S.; Shin, Y. S.; Toth, L. M.; Barnes, C. E. *Inorg. Chem.* **1997**, *36*, 4900–4902.

(7) (a) Hopkins, T. A.; Berg, J. M.; Costa, D. A.; Smith, W. H.; Dewey, H. J. *Inorg. Chem.* **2001**, *40*, 1820–1825. (b) Sornein, M.-O.; Cannes, C.; Le Naour, C.; Lagarde, G.; Simoni, E.; Berthet, J.-C. *Inorg. Chem.* **2006**, *45*, 10419–10421. (c) Gaillard, C.; Chaumont, A.; Billard, I.; Hennig, C.; Ouadi, A.; Wipff, G. *Inorg. Chem.* **2007**, *46*, 4815–4826. (d) Nockemann, P.; Servaes, K.; Van Deun, R.; Van Hecke, K.; Van Meervelt, L.; Binnemans, K.; Göller-Walrand, C. *Inorg. Chem.* **2007**, *46*, 11335–11344.

(8) Where the diffusion coefficients of $\text{U}^{\text{VI}}\text{O}_2\text{Cl}_4^{2-}$ and its reductant were assumed to be equal.

(9) Ruipérez, F.; Danilo, C.; Réal, F.; Flament, J.-P.; Vallet, V.; Wahlgren, U. *J. Phys. Chem. A* **2009**, *113*, 1420–1428.